INSTRUMENTED TECHNOLOGICAL SPECIMEN (ITS): CURING PROCESS AND MECHANICAL CHARACTERISATION USING EMBEDDED FIBRE BRAGG GRATINGS

M. Mulle[1&2], F. Collombet[1], J.N. Perié[1], Y.H. Grunevald[2]

1: Laboratoire de Génie Mécanique de Toulouse, Institut Universitaire de Technologie Paul Sabatier, 133 avenue de Rangueil, 31077 Toulouse cedex 4, France.
2: D.D.L. Consultants, Pas de Pouyen, 83330 Le Beausset, France.

ABSTRACT

A technological demonstrator is developed within the framework of the AMERICO research program (Analyses Multi-Echelles: Recherches Innovantes pour les COmposites) and in collaboration with DDL Consultants company. It's a composite material specimen, representative of industrial structures and instrumented with embedded optical fibre sensors. After having described the characteristics of the ITS, we first present the results of a cure monitoring. We then present a comparative study of three metrologies used at the same time during a three point bending test. Finally, measurements are confronted with the results of a numerical model. Some differences are observed and a discussion on their origin is proposed.

1. INTRODUCTION

Designers have to face today's complex transportation needs: fuel savings, design flexibility and high performance at lower costs. As they are durable, lightweight and corrosion resistant, composites constitute a good alternative. Nevertheless the developments of such solutions are generally limited by the lack of knowledge about the performances of these materials in real industrial situations. On the basis of this report the French research program AMERICO (multi-scale analysis of composite structures) was launched.

At the same time, a methodology elaborated through a partnership between DDL Consultants Company and the LGMT PRO²COM was proposed [1] to facilitate the characterization, the durability prediction and the certification of primary composite structures while taking into account cost reduction. One of its major concept is the ITS. It is based on the specific advantage of composite materials, i.e. they are able to be instrumented with embedded sensors. The use of fibre Bragg gratings (FBG) optical sensors in structures is a promising step to contribute to an optimal survey of composite structures throughout their life cycle. An ITS is a composite demonstrator which, on one hand, has a geometry close to a structural primary element one (i.e. containing design singularities and large dimensions), and on the other hand, is instrumented with embedded sensors. From the multi-scale approach of our methodology, the ITS concept was approved and now developed within the framework of the AMERICO upstream research program.

This paper gives a detailed description of the ITS and presents the results of a preliminary series of process and mechanical characterizations. First, a process monitoring technique with FBG's was defined and tested. The various phases of the curing process were identified and residual cure strain observed at the sensor localization was quantified. To proceed, a three point bending test has been performed. Three kinds of strain measurements were carried out at the same time and in the same region: FBG, gauges (at the vertical of FBG) and stereo Digital Image Correlation (DIC) on the top and lateral surfaces. Bragg gratings allow mesoscopic and internal measurements while the DIC method leads to a field of measures obtained on the surface of the tested specimen and representative of the macro scale. This test consists in establishing a comparison between the various metrologies applied in the core of the material as well as on the surface, in two zones of singularity which are the reinforcement zone and the drop off zone [2].

A first simulation/test comparison was achieved for a given vertical displacement assuming a classical beam kinematics. Some differences are observed. They may result from the influence of the FBG/composite interface, material properties identification (real ply thicknesses, inter ply

characteristics, initial state…) or an inappropriate kinematics description. This has yet pointed out the importance of feeding the finite element analysis with more realistic models and values. The association of the different measurement techniques and simulations will hopefully help to determine relations between the mesoscopic and the structural scales.

2. THE INSTRUMENTED TECHNOLOGICAL SPECIMEN

2.1. Composite material

The ITS is made with UD carbon / epoxy prepreg and cured in the autoclave. The selected prepreg is a material developed by Hexcel company (reference: M21 / 35% / 268 / T700GC) and used in the AIRBUS A380 program. After being cured in an autoclave, the composite material features excellent toughness at high energy impact, high residual compression strength after impact, good hot-wet properties up to 150°C, and a simple cure schedule (rise in temperature 2°C/minute up to 180°C, 120 minutes of temperature stage, and cooling down, 7 bar of pressure and -0.7 bar of vacuum pressure).

2.2. Geometry and stacking sequence

The geometrical characteristics of this demonstrator are representative of industrial design singularities and moreover, are combined on a same structural part. Singularities such as drop off, important thickness (9 to 18 mm) and large dimensions (800 x 80 mm) are included (cf. figure 1). Drilled holes filled or not, are envisaged for a future study however the first series of experiment presented here don't include this problematic.

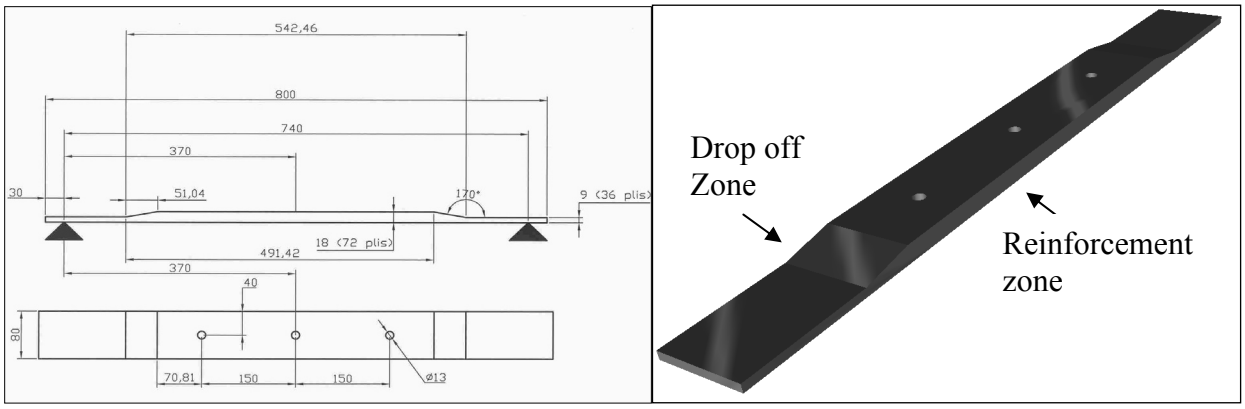

Figure 1. Plan (on left) and scheme (on right) of the technological specimen

Although the process parameters are sticking to the suppliers specifications, the stacking sequence and the layers placement are specific to our project. The specimen is made of:

- 36 plies in the current part (9 mm thick); stacking sequence: $[0/45/0/-45/0/90/\ 0/45/0/-45/0/90/0/45/0/-45/0/0]_s$;
- 72 plies in the reinforced zone (18 mm thick); the complementary stacking sequence is the same as above.

This leads to the following distribution: 55.6 % at 0°, 33.3 % at +/- 45° and 11.1 % at 90°.

2.3. Embedded instrumentation

The instrumentation of the specimen consists in embedding FBG sensors in between prepreg layers during the stacking operation (cf. figure 2). The heat resistance and the low intrusive aspect of this sensor enable precise internal measurements without significantly affecting the material properties.

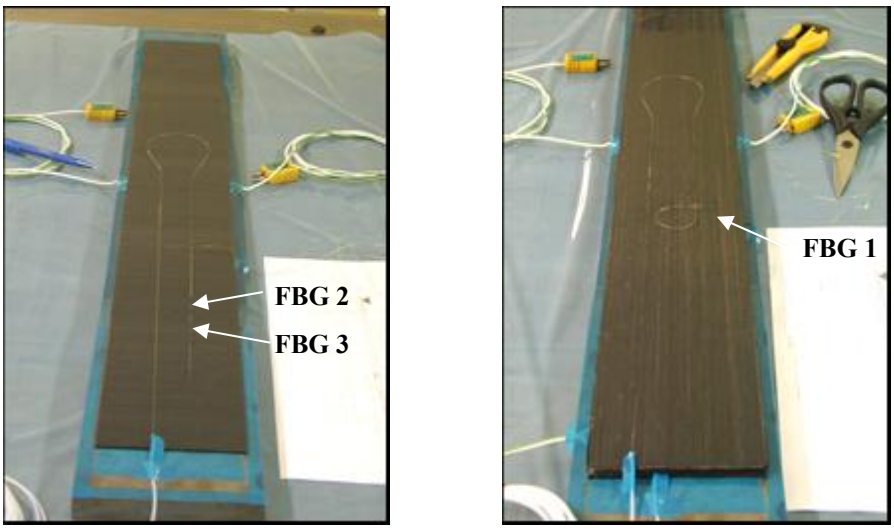

(a) (b)

Figure 2. Embedment of the 2 OF with 2 Bragg gratings: (a) between ply 30 at 90° and ply 31 at 0°; (b) between ply 12 at 0° and 13 at 90°

FBG's are exploited as sensors in many industrial fields [3] like geology, naval, aeronautics [4], railway [1] or wind energy. They have already been described in various papers since the last decade. We just remind that they are sensitive to temperature (T), strain (ε), and to hydrostatic pressure (P). FBG's deliver information which are related to a variation of the Bragg wavelength as shown in Eq. 1 (a, b, c are known constants) [5]:

$$\frac{\Delta\lambda_B}{\lambda_B} = a\Delta T + b\varepsilon + c\Delta P \quad (1)$$

As regard to our manufacturing processes and characterizing systems, we have found that the pressure influence was not significant compared to the other factors. Thus, it is considered to be negligible.

3. PROCESS CHARACTERIZATION WITH FBG'S

The curing process is monitored in order to determine the initial state of the structure. Our project is to quantify and to define the distribution of the residual strains in the cure part depending on parameters such as cooling rate, type of realising agent, internal pressure of the autoclave [6]. The use of fibre Bragg gratings seems to be a very efficient solution to undertake this characterization task as these sensors resist to high temperatures and may be embedded inside the composite material.

Our first attempt at characterizing the curing process concerned the ITS. Thermocouples were placed close to the Bragg gratings in order to collect the temperature information. We could intend to determine, at any moment of the cure process, the temperature component from the equation 1, and therefore estimate in real time the strain value (hydrostatic pressure being negligible) using Eq. 2:

$$\varepsilon = \left(\frac{\Delta\lambda_B}{\lambda_B} - a\Delta T \right) \times b^{-1} \quad (2)$$

For some reasons related to the complex information and loading conditions the results were not satisfying. The procedure to characterize the cure process needs a more complex preparation. We explain below the different steps to be taken into account and the results of a cure monitoring of a simple plate whose material is identical to that used for the technological specimen (Hexply prepreg T700/M21) but with a unidirectional stacking sequence $[0°]_{10}$.

The autoclave needs to be equipped with a specific gate in order to connect the OF to the interrogative unit (cf. figure 3 a, b). As we said above, the response of the sensor is mainly dependent on temperature and axial strain. In order to just measure the effect of axial strain we need to have a temperature compensated sensor system. To isolate and define the influence part of the temperature, we use a technique of an encapsulated FBG (cf. figure 3).

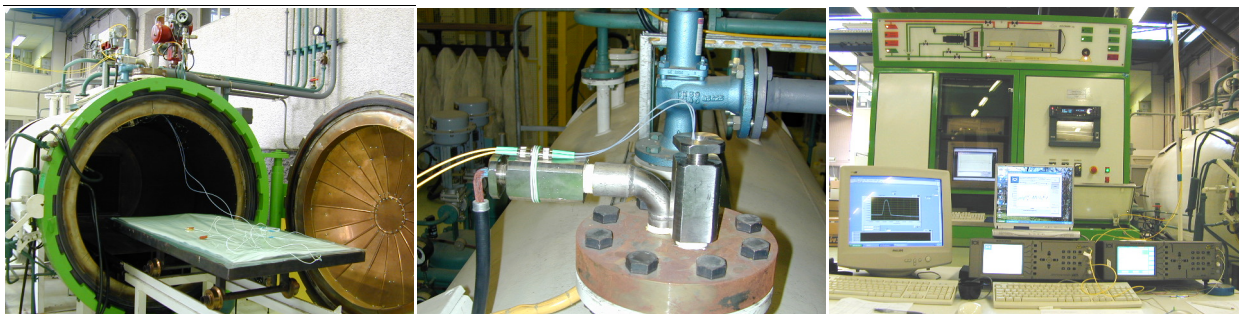

(a) (b) (c)

Figure 3. (a) LGMT autoclave; (b) OF gate; (c) acquisition systems: Micron Optics wavelength meter and swept laser OSA

In this manner, the FBG inside the hermetical needle is free of mechanical strains. A second FBG put nearby, will be sensitive to both temperature and strain. If the first FBG information are subtracted to the second FBG information, it is then possible to deduce the only mechanical action of the external environment over the second FBG. Concerning this embedded FBG we have made some observations through a BEM and noticed that to optimize the effective transfert of the matrix properties it was important to remove the protective coating around the sensor. Indeed, in case of using standard SMF28 polyacrylate coating fibre optic (250 µm), a very poor adhesion between the cladding of the fibre and the coating was created during curing (cf. figure 4c) and the collected information at the sensor's place would not represent the behaviour of the composite [9].

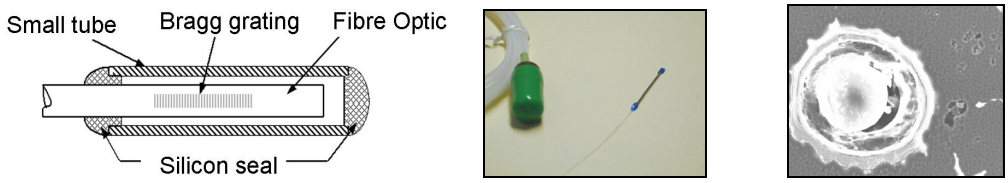

(a) (b) (c)

Figure 4. a) Scheme; b) Photo of an encapsulated FBG; c) Section of a polyacrylate coated OF in carbon/epoxy composite observed through BEM

However, some non axial strains may be encountered during the manufacturing process and may affect the answer of the FBG [7]. To minimize this effect it is important to position the FBG's in the same direction as the fibre reinforcements and if possible in the same direction of the loading. Moreover, the monitoring of the wavelength sprectrum shape using an OSA (Optical Spectrum Analyser) allows to check if the sensors are subjected to non axial or non uniform strain [8].

Having taken all the necessary cares we have monitored the autoclave process of the unidirectional plate. Figure 5 shows three wavelength spectrum shapes collected (with an si720 Micron Optics OSA) at the beginning , the middle and the end of the cure cycle corresponding to 2 FBG's written on the same optical fibre (cf. figure 5). The second FBG is encapsulated. We can observe that no division or flattening of the spectrum shapes occurred. We only show here 3 pairs of spectra but many more have been collected that relate the same behaviour. Indeed, even

after pressure and vacuum took place or during the cooling down phase, the spectra kept a clear single peak shape. We observe 2 variations: a peak shift due to temperature variation and/or axial strain and also an attenuation of the signal power due to phenomena such as micro-bendings which are taking place along the embedded optical fibre.

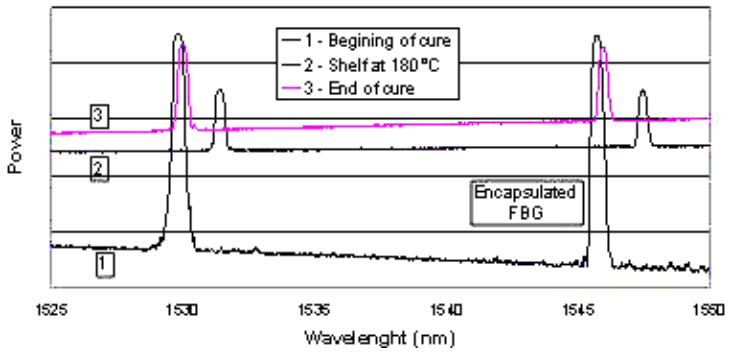

Figure 5. Three wavelength spectrum shapes collected during an autoclave cure process

As we are now more confident in the nature of the information collected by the FBG's we may recall the evolution of strain at the location of the non-encapsulated sensor during the cure cycle. The si425 Micron Optics swept laser interrogator acquires in real time the peak shift variations which are proportionally related to the evolution of temperature and/or strain. Being able to determine the temperature component in Eq.2 thanks to the encapsulated FBG we evaluate the longitudinal behaviour of the prepreg along the cure cycle. At the end of the cooling down phase we may estimate a residual strain of 90µm/m.

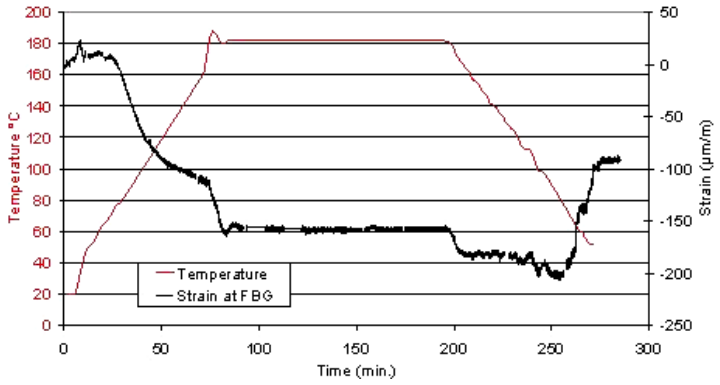

Figure 6. Longitudinal response of $[0°]_{10}$ prepreg T700/M21 during autoclave curing process

4. MECHANICAL CHARACTERIZATION

The technological specimen was subjected to three point bending tests (cf. figure 7), carried out at constant speed, up to a loading of 10 kN. Three kinds of metrologies are used, conventional strain gauges, digital images correlation (DIC) and Bragg grating measurements. Bragg gratings allow mesoscopic and internal measurements while the DIC method leads to a field of measures obtained on the surface of the tested specimen and representative of the macro scale. This test consists in establishing a comparison between the metrologies in two zones of singularity which are the reinforcement zone and the drop off zone [2].

The first test aims at validating strain measurements on the surface. The second allows comparing internal and surface metrologies in a cross-section of the reinforcement zone. The third test enables to compare measurements obtained in the drop off zone.

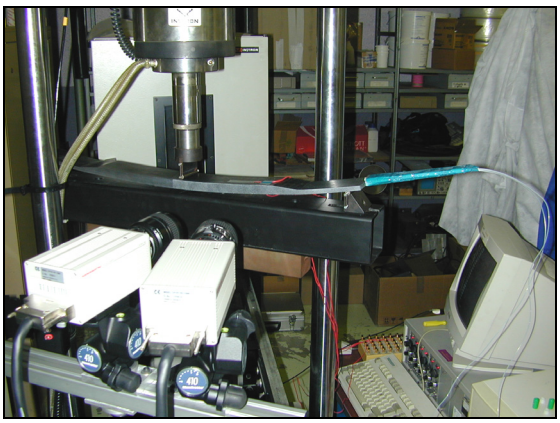

Figure 7. Three point bending test carried out on a multi-instrumented technological specimen

In spite of the important dimensions of the specimen, the tests are carried out on a dynamic mechanical testing machine of INSTRON type whose maximum force is of ± 100 kN and the useful race of ± 50 mm. Strain measurements are gathered by electric gauges with a VISHAY extensometry bridge. Field measurements are obtained by stereo-correlation of digital images, using two CCD Hamamatsu numerical cameras. The numerical image processing is carried out with the assistance of the commercial software Vic3d© (Correlation Solution, Inc).
With regards to measurements by Bragg gratings, they are carried out with the si425 Micron Optics unit. It is supposed that the conditions of test are isothermal. We can then directly estimate strain using the following simplified equation (Eq. 3):

$$\varepsilon = \frac{\Delta\lambda_b}{a\lambda_b} \tag{3}$$

4.1. Position of the measurement points

We are mainly interested in observing two zones of singularities (cf. figure 8):
- the reinforcement zone on which a number of sensors is laid out according to a section perpendicular to the specimen axis, at 150 mm from the center. First, an observation will be carried out on the top face of the specimen, then on the side;
- the drop off zone for an observation on the section.

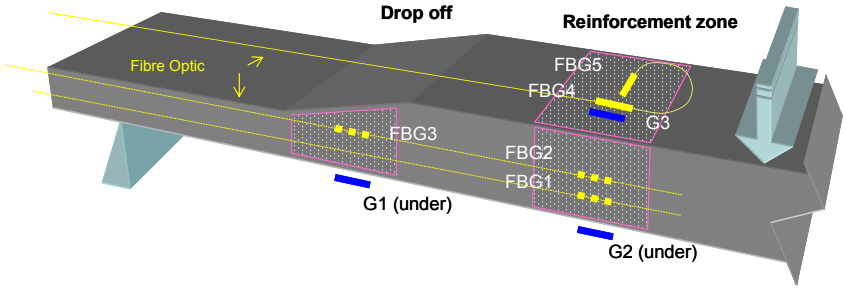

Figure 8. Position of all the sensors and measured fields on the ITS

At the time of the laying up, a first Bragg grating (FBG2) is integrated in between plies 30 and 31 respectively oriented at 90° and 0°. A second grating (FBG1) is integrated in between the plies 12 and 13 respectively oriented at 0° and 90° (cf. figure 2). Two extensometric gauges are stuck to the right of the FBG: J2 on the lower face and J3 on the top face. On the latter, an FBG (FBG4) is stuck parallel to the J3 gauge and another FBG (FBG5) perpendicularly. With the exception of the FBG5 all the sensors are laid out so as to measure a deformation along the principal axis of the specimen.

4.2. Comparison of metrologies on the top face in the reinforcement zone

For this test, the cameras shoot the top part of the specimen. On this face, a strain gauge (J3) and two FBG's (FBG4 and FBG5) are stuck. The field measurement on the zone where the sensors are laid out allows checking the homogeneity of the deformations (cf. 9a). We do not observe any particular incidence of the gluing of the optical fibres on the measured strains.We can then carry out a direct comparison of the measurement provided by all three metrologies (cf. figure 9b).

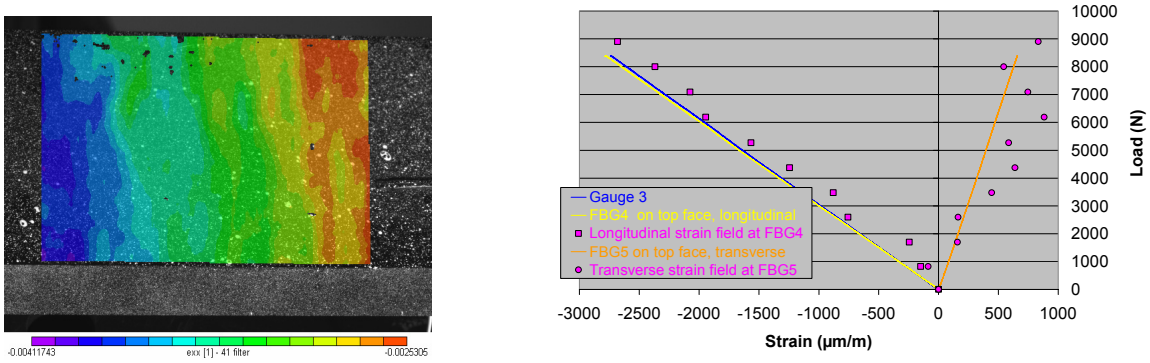

(a) (b)

Figure 9. a) Longitudinal strain displacement field ε_{11} on the top face of the ITS measured at load of 8 kN; b) Gauge, FBG and DIC strain evolution ε_{11} et ε_{22} measured on the top face of the ITS in the reinforced zone

We observe a very satisfactory accordance (less than 2% of variation) between the longitudinal measurements taken by the J3 gauge and the Bragg grating FBG4 (cf. figure 9b). The reliability of measurement being shown, we can evaluate the Poisson's ratio by using the information of FBG4 (longitudinal direction) and FBG5 (transverse direction): ν_{12} = 0,236. Field measurements are dispersed, letting appear differences with the other sensors of approximately 10 % in the longitudinal direction and nearly 25% in the transverse direction. Field measurements present a systematic error which can be explained by the low level of strain measured and by a limited resolution of 10^{-4}.

4.3. Comparison of measurements taken in the thickness of the reinforcement zone

It is a question of comparing the evolution of internal strain measurements (FBG) with those carried out on the side face of the specimen, at the same height by Digital Images Correlation (DIC). The longitudinal strain field ε_{11} measured on the side face by DIC is presented in figure 10a. The figure 10b shows the evolution of FBG strain measurements and field measurements at various stages of the loading. An excellent agreement is observed in the case of the FBG1. The results relating to the FBG22 are less significant. However the difference between measurements does not exceed 10%.

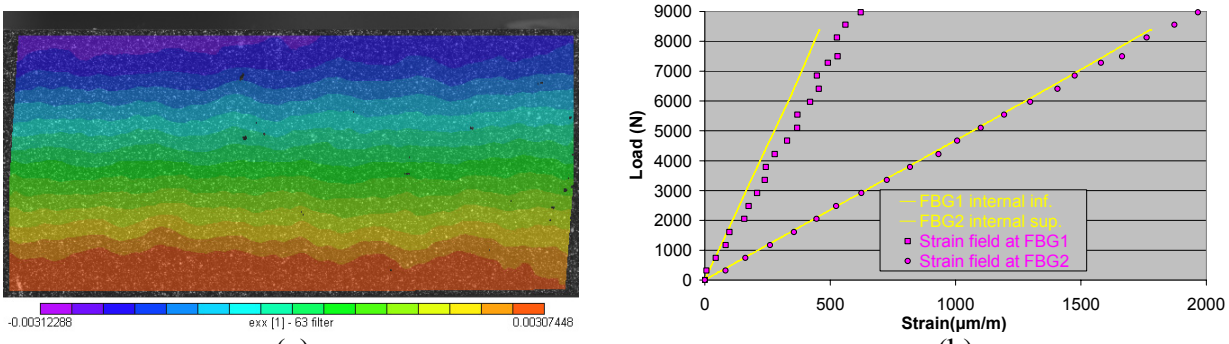

(a) (b)

Figure 10. a) Longitudinal strain field ε_{11} measured on the side of the reinforced zone at a load of 8 kN; b) FBG and DIC strain evolution ε_{11} on side of the reinforced zone

4.4. Measurements taken in the thickness of the drop off zone

The objective of this test is to validate internal metrology in a more singular area from the point of view of its geometry. In this area, an FBG is placed in the core of the material , and a gauge is stuck on the lower face, below the FBG (cf. figure 8). The figure 11a shows the strain distribution ε_{11} measured by DIC on the side of the specimen. These values are compared with the FBG and gauge measurements. A great similarity is observed, in spite of the relative complexity of the area in which these measurements are taken (cf. figure 11b).

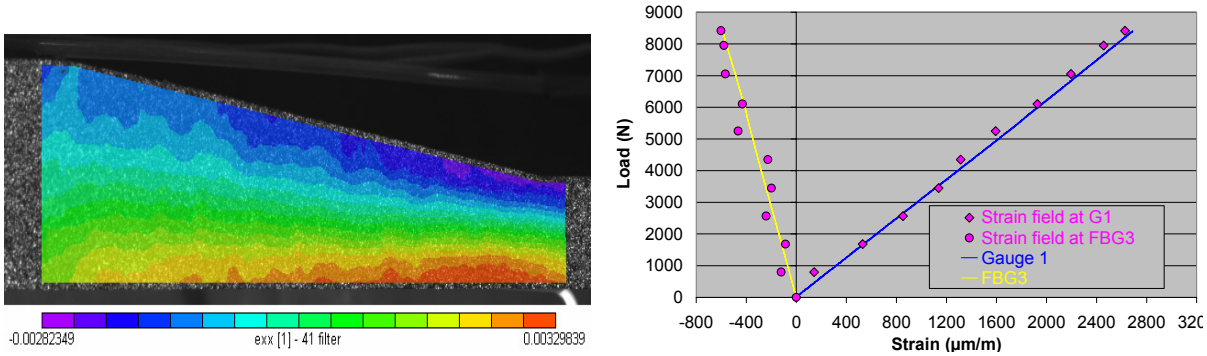

(a) (b)

Figure 11. a) Field of longitudinal strains ε_{11} measured on the side face at a load of 8 kN;
b) Gauge, FBG and DIC strain evolution ε_{11} on the drop off zone.

5. TEST/CALCULATION COMPARISON

5.1. Numerical modelling

The ITS is modelled with SAMCEF software. For the test/calculation comparison, the 3 point bending test is modelled by imposing a displacement on the nodes so as to the value is equal to the displacement measured at the time of the tests.

5.2. Comparative results

The section considered is rather far from the drop off and the boundary conditions. The various values measured or calculated in the cross-section (FBG, gauges, DIC, numerical model) are confronted for a given displacement (27,5 mm) by considering a Timoshenko kinematics. A graphic construction is proposed to compare the values: a line connecting the calculated deformations is traced in figure 12. It allows estimating the distribution of the internal strains. The general tendency is that expected. Experimental internal and surface measurements are in accordance with the numerical simulation even though some variations are noticed (approximately 5%).

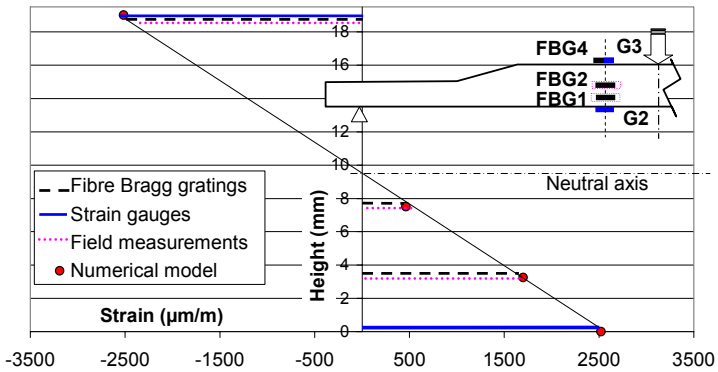

Figure 12. Comparison of measurements (FBG, gauges, DIC, model) taken in a cross-section concerning a 3 point bending test

5.3. Process parameters

The simulation shows a satisfactory correlation with experimental results. However, a difference of rigidity appears between calculations and tests. This may be due to the variability of parameters directly related to the manufacturing process. Among them are parameters such as ply thickness, inter-ply nature or residual strains.

The observation of an elementary specimen sample with a BEM (cf. figure 18) shows the thickness variability of the plies. After laying up and polymerization of the elementary specimen, we measure a 2.21 mm total thickness. If we carry out a simulation according to the data of supplier HEXCEL Composites (ply thickness = 0.26mm), we find a 2.08 mm total theoretical thickness that is to say a 0.13 mm difference with the measured value. This difference can thus have a real influence on the rigidity of the specimen (since it exploits the moment of inertia and/or the fiber content ratio). Therefore, the plies are not distributed uniformly. 0° plies have a thickness higher than the one given by the supplier and the tendency is reversed with the 90°plies. The values lie between 0.243 mm and 0.314 mm.

By BEM observation, it is also possible to see the presence of nodules in the inter plies rich in resin (cf. figure 13). The nodules are thermoplastic microballs which have a function to slow down the crack propagations and to improve the impact behavior. Their concrete influence on the elastic behavior of the structure is not identified yet. A thorough study of these interfaces is in progress. The objective of this work is to define a model adapted to this entity.

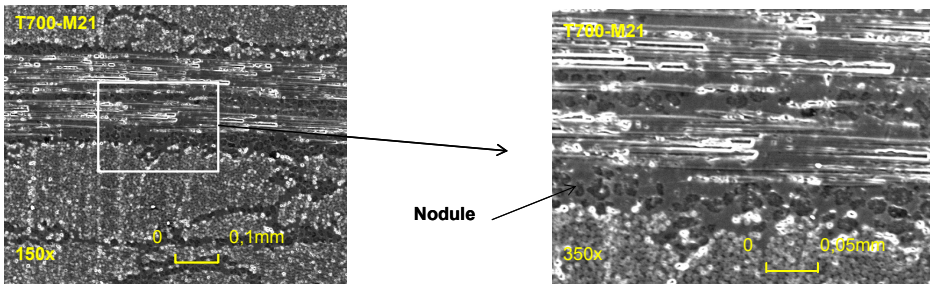

Figure 13. BEM observations at the interface of two crossed plies (0°,90°) of T700/M21 (zoom on right)

We have shown above the existence of longitudinal residual strains in a UD carbon/epoxy part after curing in an autoclave. We may suppose that the level of residual strain is much higher when the stacking sequence is more complex like in the technological specimen. The initial state of the material is strongly dependent on the process parameters. It is thus necessary to consider them when designing a composite structure.

5. CONCLUSIONS

A technological specimen instrumented with internal fibre Bragg gratings and integrating several design singularities is being developped. A test to characterize the autoclave cure cycle using embedded fibre Bragg gratings is carried out. The complexity of such experiment is shown and some solutions are proposed. The longitudinal cure strain in a UD 0° carbon/epoxy part is estimated. In a further development, we will analyze, thanks to the FBG's, the cure residual strains in a more complex stacking sequence of the same carbon/epoxy. We will also try to quantify and to define the distribution of the residual strains in the cure part by placing FBG's at different levels of the thickness and estimate the influence of the mould or the type of realising agent.

The technological specimen was subjected to a multi-instrumented three point bending test. Three kinds of metrologies are used, conventional strain gauges, displacement fields and Bragg grating measurements. Strain measurements obtained on the surface were compared and showed similar responses. Moreover, embedded measures (FBG) were validated in both zone of singularities by the surface metrologies (gauges and DIC).

The technological specimen and the three point bending test are modelized. The simulation shows a satisfactory accordance with experimental results. However, a difference of rigidity appears between calculations and tests. This may be due to the variability of parameters such as ply thickness, inter-ply nature or residual strains. We will continue to analyze these parameters and others in order to obtain a more representative model of the macroscopic behaviour of the specimen.

ACKNOWLEDGEMENTS

The authors wish to thank Dr. Laurent Robert from the EMAC (CROMeP) for his contribution to the displacement field measurements, the DGA (Direction Générale de l'Armement) for its financial support through the upstream program AMERICO controlled by the ONERA (French National Aerospace Research Establishment) and HEXCEL Composites company for the provision of HexPly® pre-preg necessary to this study.

References

1. **Grunevald, Y.H., Collombet, F., Mulle, M.** and **Ferdinand P.**, "Global approach and multi-scale instrumentation of composite structures in the field of transportation", *Proceedings of 8th Japan Int. SAMPE*, Tokyo (Japan), Nov. (2003).
2. **Mulle M., Périé, J.N., Collombet, F., Robert, L.** and **Grunevald, Y.H.**, "Mesures de champs sur éprouvette technologique instrumentée par réseaux de Bragg : comparaison et validation de métrologies" (in french), *Colloque Photoméca,* Albi (France) (accepted for oral presentation), (2004).
3. **Bugaud, M.** and **Ferdinand, P.**, "Mesures de micro déformations par capteur à fibre optique à réseaux de Bragg", *LETI CETIM*, Senlis (France), (2000).
4. **Esquer, P.M., Lence, F.R.** and **Menendez, J.M.**, "Optical fibre sensors in AIRBUS Spain", *Structural Health Monitoring*, Paris (France), July (2002).
5. **Ferdinand, P.**, "Capteurs à fibres optiques à réseaux de Bragg"; *Techniques de l'Ingénieur, traité Mesures et Contrôle*, **R 6 735-1**, Dec. (1999).
6. **Tarsha Kurdi, K.E.**, "Contraintes résiduelles de cuisson dans les stratifiés composites à finalité aéronautique : intégration du procédé de mise en œuvre et étude de leur influence sur les caractéristiques mécaniques", *Thèse de l'Université P. Sabatier (PhD thesis report in french)*, Toulouse (France), (2003).
7. **Takeda, N.**, "Structural health monitoring for smart composite structure systems in Japan", *Ann. Chim. Sci. Mat.*, (2000), 545-549.
8. **Kang, H.K.** et al., "Monitoring of fabrication strain and Temperature during composite cure using fiber optic sensor", *SPIE,* Vol. **4336**, (2001).
9. **Yuan L.** et al., "Investigation of a coated optical fiber strain sensor embedded in a linear strain matrix material", *Optics and Lasers in Eng.*, **35**, (2001).